OMI Satellite Observations of decadal changes in Ground-Level Sulfur Dioxide over North America

Shailesh K. Kharol[1], Chris A. McLinden[1], Christopher E. Sioris[1], Mark W. Shephard[1], Vitali Fioletov[1], Aaron van Donkelaar[2], Sajeev Philip[2], Randall V. Martin[2]

[1]Air Quality Research Division, Environment and Climate Change Canada, Toronto, Ontario M3H 5T4, Canada
[2] Department of Physics and Atmospheric Science, Dalhousie University, Halifax, Nova Scotia, Canada

Correspondence to: S. K. Kharol (shailesh.kharol@canada.ca)

Abstract. Sulfur dioxide (SO_2) has a significant impact on the environment and human health. We estimated ground-level sulfur dioxide (SO_2) concentrations from the Ozone Monitoring Instrument (OMI) using SO_2 profiles from the Global Environmental Multi-scale – Modelling Air quality and CHemistry (GEM-MACH) model over North America for the period of 2005-2015. OMI-derived ground-level SO_2 concentrations (r = 0.61) and trends (r=0.74) correlated well with coincident in-situ measurements from air quality networks over North America. We found a strong decreasing trend in coincidently sampled ground-level SO_2 from OMI (-81±19%) and in-situ measurements (-86±13%) over Eastern US for the period of 2005-2015, which reflects the implementation of stricter pollution control laws including flue-gas desulfurization (FGD) devices in power plants. The spatially and temporally contiguous OMI-derived ground-level SO_2 concentrations can be used to assess the impact of long-term exposure to SO_2 on the health of humans and the environment.

1 Introduction

Sulfur dioxide (SO_2) is a short-lived atmospheric trace gas emitted into the atmosphere from natural (e.g. volcanic eruption, oxidation of dimethylsulphate (DMS) over oceans) and anthropogenic sources (e.g. combustion of fossil fuels and smelting of sulfur-containing metal ores), and plays a pivotal role in the global sulfur cycle. SO_2 has a short lifetime of hours to days, and it oxidizes quickly in the atmosphere to produce sulfate aerosols that affect the climate (Intergovernmental Panel on Climate Change, 2013) and the environment from local to regional and global scales. Sulfate aerosols are major contributor to $PM_{2.5}$ (particulate matter with aerodynamic diameter < 2.5 μm) chemical composition and accounts for 17% and ~30% of the annual mean $PM_{2.5}$ mass globally and over eastern United States (Philip et al., 2014). Sulfate aerosol formation leads to degradation in visibility and air quality (van Donkelaar et al., 2008), deposition of sulfuric acid (Dentener, et al., 2006; Vet et al., 2014), and poses a serious health hazard to the general population (Lee et al., 2015). The increased risk of premature mortality associated with SO_2 alone or its secondary pollutants has been emphasized in several epidemiological studies (Chinn et al., 1981; Derriennic et al., 1989; Hatzakis et al., 1986; Krzyzanowsli & Wojtymiak, 1982). Furthermore, it has been recently reported by Lelieveld et al., (2015) using the EMAC (ECHAM5/MESSy Atmospheric Chemistry) general circulation model that in the U. S., in addition to agricultural emissions (an important source of ammonia (NH_3)), emission

from coal fired power plants (an important source of SO_2 and nitrogen oxides (NO_x)) is the largest contributor to premature mortality in 2010. Due to the adverse impact on the environment and human health, SO_2 and its oxidation products (i.e. fine particulate matter ($PM_{2.5}$)) are considered as designated criteria pollutants in European Union (European Commission, http://ec.europa.eu/environment/air/quality/standards.htm), United States of America (US Environmental Protection Agency (EPA), https://www.epa.gov/criteria-air-pollutants) and Canada (https://www.ec.gc.ca/Air/default.asp?lang=En&n=7C43740B-1).

Globally, atmospheric SO_2 is monitored regularly through a relatively small number of measurement networks, that produce accurate measurements, but over a limited spatial area. Satellite measurements have the advantage of providing complete daily global coverage of SO_2. Satellite observations of SO_2 vertical column density (VCD) begun in the 1980s but the launch of the Ozone Monitoring Instrument (OMI) (Krotkov et al., 2006, Yang et al., 2007) on the Aura satellite in 2004 has enabled large point sources to be resolved with its higher spatial resolution (13 x 24 km^2 at nadir) (Fioletov et al., 2013). Satellite measurements of SO_2 have been used to identify and analyze emissions (Fioletov et al., 2011, 2013, 2015, 2016; Lee et al., 2011; McLinden et al., 2016a), track changes in total column density in various regions including Canadian oil sands, eastern US, eastern Europe, eastern China, India and Middle East (McLinden et al., 2016b; Krotkov et al., 2016), and estimate dry deposition flux (Nowlan et al., 2014). In previous studies (Lee et al., 2011; Nowlan et al., 2011), ground-level SO_2 concentrations were estimated for only a one year period using satellite observations over North America. However multi-year spatial variations in ground-level SO_2 have not yet been assessed from the satellite observations. In contrast to total column SO_2, long-term records of ground-level SO_2 concentrations from satellite observations will be directly useful to assess air quality and associated health risks. Recently, a decreasing trend in SO_2 emissions and particulate sulfate has been reported by Hand et al. (2012) over the United States from the early 1990s through 2010.

In this paper we first describe the OMI SO_2 product, in-situ measurement network, the GEM-MACH (Global Environmental Multi-scale – Modelling Air quality and Chemistry) air quality model, ground-based SO_2 estimation from OMI and trend analysis. We then use these data and methodology to estimate ground-level SO_2 from OMI and evaluate it with coincident in-situ measurements over North America for the period of 2005-2015. These results are then used to determine the trend in ground-level SO_2 from both OMI and collocated in-situ measurements.

2 Data sets & methodology

2.1 OMI

OMI is a nadir-viewing UV-visible spectrometer boarded on the Aura satellite that was launched in July 2004, and is part of the NASA A-train constellation (Levelt et al., 2006). The Aura satellite overpasses the equator at early afternoon (1300-1430 local time) in sun-synchronous ascending polar orbit. OMI provides daily global coverage of aerosols and trace gases,

including SO_2, with a variable ground spatial resolution of 13 km × 24 km at nadir to 140 km × 26 km at swath edge. We use the OMI operational Principal Component Analysis (PCA) SO_2 product (OMSO2 v1.2.0), which is publically available from NASA Goddard Earth Sciences (GES) Data and Information Services Center (DISC) (http://disc.sci.gsfc.nasa.gov/Aura/data-holdings/OMI/omso2_v003.shtml). The details of PCA algorithm can be found elsewhere (Li et al., 2013). In brief, this algorithm applies the PCA technique to OMI-measured radiances between 310.5 and 340 nm to extract principal components from each row of data on an orbital basis. The PCA algorithm replaced the Band Residual Difference (BRD) algorithm (Krotkov et al., 2006) as the operational algorithm for the standard OMI SO_2 data because only the latter algorithm was biased (Fioletov et al., 2013; Krotkov et al., 2016). Also, SO_2 retrieval variability is reduced by a factor of two in the PCA algorithm relative to the BRD algorithm (Li et al., 2013). Even though the PCA algorithm directly estimates SO_2 vertical column density in one step using SO_2 Jacobians, the air mass factor (AMF) is effectively fixed at 0.36 (representing summertime conditions in the eastern USA), similar to the BRD algorithm. A better estimation of AMFs is needed for different regions to reduce these systematic errors that result from conditions that do not match these. For this, we re-calculated the AMFs using SO_2 profile information from the high resolution (15 km x 15 km) GEM-MACH air quality forecast model (discussed in section 2.3), monthly-varying surface reflectivity from the MODIS satellite instruments, and an improved identification of snow. More details on Environment Canada Air Mass Factors calculation for SO_2 are discussed in McLinden et al., 2014; 2016b. Here, we exclude the cross-track pixels affected by the row anomaly (http://www.knmi.nl/omi/research/product/rowanomaly-background.php), which was first noticed in the data in June 2007. We use OMI SO_2 columns with cloud radiance fraction <0.2, and solar zenith angles $<65^o$ following Nowlan et al. (2014). We exclude from the analysis the OMI SO_2 data affected by the largest northern mid-latitude volcanic eruptions in the OMI time frame namely Kasatochi (Aleutian Islands, Alaska, August 2008, 52^oN) and Sarychev (Kuril Islands, Eastern Russia, June 2009, 48^oN). Here, we used the mean OMI values over a 32 km averaging-radius (Fioletov et al., 2011) that is oversampled onto a 0.1° x 0.1° latitude/longitude grid.

2.2 SO_2 monitoring networks

To evaluate the OMI-derived ground-level SO_2 we use hourly in-situ SO_2 measurements from the Air Quality System (AQS) network of the US EPA (http://www.epa.gov/ttn/airs/airsaqs/detaildata/downloadaqsdata.htm) and Environment and Climate Change Canada's National Air Pollution Surveillance (NAPS) network (http://maps-cartes.ec.gc.ca/rnspa-naps/data.aspx) over the US and Canada for the period of 2005 to 2015. US-EPA AQS site locations vary from regional background to urban and industrial locations, and measures SO_2 using continuous gas monitors. The Canadian NAPS sites are generally located in populated areas. The hourly in-situ measurements are averaged over a 2 h period (1300-1500 Local Time) to correspond with the satellite observation times over North America.

2.3 Model information

We use the Global Environmental Multi-scale – Modelling Air quality and CHemistry (GEM-MACH) model for the tropospheric SO_2 profile to relate the OMI SO_2 column to ground-level concentrations. GEM-MACH is the Canadian regional air quality forecast model used operationally to predict the concentrations of O_3, NO_2, and $PM_{2.5}$ over North America (Moran et al., 2010, Gong et al., 2015). GEM-MACH model utilizes emissions inventories from US EPA and Environment Canada data for the year 2006. It uses detailed tropospheric processes for gas and particle chemistry and microphysics originating in the offline AURAMS model (A Unified Regional Air-quality Modelling System; Gong et al., 2006), and incorporates them on-line into the Canadian weather forecast model (Global Environmental Multiscale model, Côté et al., 1998). A detailed description of the chemical processes found in AURAMS and GEM-MACH is provided elsewhere (Kelly et al., 2012). The results used here are from archived forecasts from 2010 to 2011 for a domain covering North America at 15 km×15 km resolution. The lowest model layer, which is 20 m thick, is taken as ground-level concentration.

2.4 Estimation of ground-level SO_2 from OMI

The ground-level SO_2 mixing ratio from OMI is estimated using the approach described by Lamsal et al. (2008) over North America for the period of 2005-2015. The ground-level SO_2 mixing ratio S is estimated from the local OMI tropospheric SO_2 column Ω as:

$$S_{OMI} = \Omega_{OMI} \times \frac{S_{model}}{\Omega_{model}} \quad (1)$$

The subscript $model$ represents GEM-MACH model. More details on the procedure are discussed in McLinden et al. (2014).

2.5 Trend Analysis

We analyzed the trends in monthly ground-level SO_2 over North America from OMI and in-situ measurements for the period of January 2005 - December 2015. We applied a general least squares regression following Boys et al. (2014) and Kharol et al. (2015) using the basic model:

$$x = z\beta + e, \quad e \sim N(0, \sigma^2 V) \quad (2)$$

where, for a time series of n months, x is a time series vector (n × 1) containing SO_2 surface mixing ratio values; z is a design matrix (n × 2) for the linear model; β is a vector (2 × 1) containing the intercept and slope of the linear model; e is an error vector (n × 1) containing the residuals which, for validity, should be approximately normally distributed with zero mean, however, is permitted to covary with adjacent values according to V – a positive definite, symmetric covariance matrix, to accommodate possible autocorrelation between adjacent months. Correlated errors between adjacent months are represented by a first order autoregressive model of e, which can be expressed as:

$$e_t = \emptyset e_{t-1} + w_t \qquad t = 1, \ldots n,\ w \sim N(0, \sigma^2 I) \tag{3}$$

where, the residual e_t for month t is a fraction $\emptyset$ of the previous month's residual e_{t-1} with a white noise component w_t which, for validity, should be approximately normally distributed with zero mean, constant variance and independent. We deseasonalized the monthly time series by subtracting the climatological monthly median prior to regression. Note, the trend is more heavily weighted toward summer when observations are more frequent.

3 Results & Discussion

Figure 1 shows the spatial distribution of mean OMI-derived ground-level SO_2 over North America for the periods of 2005-2007, 2008-2010, 2011-2015 and 2005-2015. The major SO_2 hotspots (that is, locations of high SO_2 associated with a large nearby source) are primarily located in the Eastern US from coal-fired power plants and industrial activities (Krotkov et al., 2016). There are far fewer sources in the western US and Canada, with a few notable exceptions such as Flin Flon (54.77^o N, 101.88^o W; copper smelter), Sudbury (46.52^o N, 80.95^o W; copper and nickel smelter), Thompson (55.74^o N, 97.85^o W; metal ore mining), Montreal (45.50^o N, 73.56^o W), the oil sands region in northern Alberta and power plants nearby Edmonton. The spatial distribution of annual mean OMI-derived ground-level SO_2 for each year is shown in supporting information Figure S1. A noticeable decrease in OMI-derived ground-level SO_2 is apparent from Figure 1 during 2008-2010 and 2011-2015 compared to 2005-2007. These US reductions correspond with the installation of flue-gas desulfurization (FGD) units at many power plants to meet stricter emissions limits introduced by the Clean Air Interstate Rule. The closure of Flin Flon (54.77^o N, 101.88^o W) copper smelter in June 2010 is also apparent in OMI-derived ground-level SO_2 during 2011-2015 (Figure 1). The OMI-derived ground-level SO_2 concentrations over large geographical area could be useful to assess its impact on human health and environment. It can also provide valuable information to policy makers where air quality network measurements are not available.

To verify these satellite findings, we compared the OMI-derived ground-level SO_2 concentrations with in-situ measurements over North America for the period of 2005-2015. The original OMI-derived ground-level SO_2 concentration (black circles) moderately correlates with collocated in-situ measurements (r = 0.61), but have a significant difference in slope (slope = 0.39) (Fig 2). The departure from unity of the slope is a common feature of virtually all satellite-surface comparisons of this kind (Kharol et al., 2015), and can be a result of both the in-situ monitor placements (i.e. mainly located in the cities and close to pollution sources) and differences in the spatial sampling of the two types of observations. To quantify this inhomogeneity effect we utilized output from the GEM-MACH model at high-resolution (2.5 km x 2.5 km; supporting information Fig S2) over a region in central Canada. These high-resolution GEM-MACH SO_2 columns at the locations of the in-situ monitors were taken as representative of point (in-situ) measurements. The model SO_2 columns were then

progressively averaged up (smoothed) to 30 km x 30 km, approximately representing the spatial size of an OMI pixel. The smoothed columns are regressed against the unsmoothed columns. The slope and correlation coefficient continue to decrease from unity as the smoothing is increased. We used this estimate of the spatial inhomogeneous sampling obtained from the original (2.5 km) vs smoothed (30 km) GEM-MACH SO_2 column (supporting information Fig S3) to derive a scaling factor (in-situ scaled = 0.52 × (in-situ) + 0.04, R = 0.83) that is used to adjust the in-situ measurements to be representative of the OMI pixel size over all of North America. We noticed ~92% increase in slope to 0.75 when comparing the spatial inhomogeneity adjusted in-situ measurements with the OMI ground-level SO_2 (red circles in Fig. 2). In comparison to previous studies, Lee et al. (2011), comparing ground-level SO_2 mixing ratios derived from SCIAMACHY and OMI with in-situ measurements from US-EPA AQS and NAPS monitoring networks over the United States and Canada for the year of 2006, reported slightly higher correlation (r = 0.86, slope = 0.91 for SCIAMACHY and r = 0.80, slope = 0.79 for OMI). In their study they used 15 km coincidence criterion and included only AQS sites measuring less than 6 ppbv at satellite overpass times. Nowlan et al., (2011) estimated ground-level SO_2 from GOME-2 and compared with in-situ measurements over North America from Clear Air Status and Trends Network (CASTNET; r = 0.85) and US-EPA AQS and NAPS (r = 0.40) for 2008.

We determined the trend in ground-level SO_2 from OMI using the monthly time series from January, 2005 to December, 2015. Figure 3 illustrates the spatial distribution of OMI-derived ground-level SO_2 trend over North America for the period of 2005-2015. We noticed a strong decreasing trend in ground-level SO_2 over eastern US and Flin Flon in Canada. The observed decrease in ground-level SO_2 concentration in the eastern US corresponds to more strict pollution control laws implemented to reduce SO_2 emissions and the installation of FGD devices in power plants (Fioletov et al., 2011; Krotkov et al., 2016). Furthermore, we estimated the trend in ground-level SO_2 at in-situ locations collocated with OMI. The upper panel of Fig 4 shows the trend in ground-level SO_2 from OMI and collocated in-situ measurements over North America for the period of 2005-2015. Both in-situ and OMI-derived ground-level SO_2 mixing ratios show a strong decreasing trend over eastern US mainly located at locations close to power plants. The lower panel of Fig 4 shows the scatter plot of trends in ground-level SO_2 from collocated in-situ measurements and OMI. The OMI-derived trends are significantly correlated (r = 0.74) with collocated in-situ trends. As expected the slope of 0.43 is similar to the absolute concentrations slope (Fig. 2) and reveals the difference in absolute trend.

Figure 5 shows the percentage change compared to 2005 in annual mean ground-level SO_2 concentration from coincidently-sampled OMI and in-situ measurements and total SO_2 emissions from power plants over eastern US. The geographical locations of stations considered over the eastern US are shown inside the blue color box within the inset map. Both OMI and in-situ measurements shows -81±19% and -86±13% decrease in ground-level SO_2 over the eastern US, respectively. Earlier OMI SO_2 columns studies reported a 40% (Fioletov et al., 2011) and 80% (Krotkov et al., 2016) decrease near power plants in Eastern US and Ohio River Valley for the period of 2005-2010 and 2005-2015, respectively. Furthermore, we derived a

decrease of 64±18% from spatially averaged OMI-derived ground-level SO_2 (Fig. 3) over the eastern US from entire domain (blue box in Fig. 5). The observed decrease in ground-level SO_2 from OMI and in-situ measurements is in agreement with the US EPA reported decrease of about 70% in total US SO_2 emissions (https://www3.epa.gov/airtrends/aqtrends.html). Figure 6 shows that bottom-up SO_2 emissions and OMI-derived ground-level SO_2 concentrations are temporally correlated even for larger individual point sources, namely the Bowen power plant (34.13° N, 84.92° W), USA, and Flin Flon copper smelter (54.77° N, 101.88° W), Canada. The bottom-up emission data for these sites are obtained from the US EPA (2016), and National Pollutant Release Inventory (NPRI, 2017), respectively.

Recently Philip et al. (2014) analyzed the $PM_{2.5}$ chemical composition over North America from the satellite data and reported that sulfate aerosols contribute ~30% in ground-level $PM_{2.5}$ mass concentration over the eastern US. Here, the ground-level sulfate $PM_{2.5}$ mass concentration is estimated by applying the sulfate fraction from Philip et al., (2014) to the total $PM_{2.5}$ mass concentration inferred using the method of van Donkelaar et al. (2010), which uses information from satellites, models and monitors. Figure 7 shows the spatial distribution of OMI SO_2 vertical column density (left panel) and sulfate $PM_{2.5}$ mass concentration over eastern US for the period of 2005-2008. The locations of large (>18.98 kt[SO2]/yr in 2006) power plants (largest contributor to SO_2 emissions) and 2005-2008 average boundary-layer winds from an ECMWF (European Center for Medium range Weather Forecasting) reanalysis (Dee et al., 2011) are overlaid on the plots as circle and arrows respectively. This demonstrates that SO_2 VCD influence air quality locally due to its shorter atmospheric lifetime. However, sulfate $PM_{2.5}$, with a longer atmospheric lifetime, influences air quality locally as well as downwind through long-range transport. It is evident from Figure 7 that column SO_2 and sulfate $PM_{2.5}$ hotspots are collocated around and downwind of power plant locations. There is only a moderate spatial correlation (r = 0.60) between OMI SO_2 and sulfate $PM_{2.5}$ but given that sulfate is largely a secondary pollutant, this is not surprising. It was also found that there is a saturation effect at high SO_2 VCDs (Supporting Information Fig S4).

4 Conclusions

We examined the spatial and temporal characteristic of the ground-level SO_2 concentration from OMI over North America during the period from 2005-2015. OMI-derived ground-level SO_2 concentrations and trend correlates well with in-situ measurements (r = 0.61 and 0.74, respectively) with a significant bias in slope. Once the in-situ observations are adjusted, based on nested GEM-MACH model results, to account for the spatial sampling differences between the in-situ and OMI spatial resolution there is a notable increase (~92%) in slope to a value of 0.75. The observed reduction in ground-level SO_2 concentration from OMI (-81±19%) is consistent with in-situ measurements (-86±13%) over Eastern US for the period of 2005-2015. The observed decreasing trend in ground-level SO_2 could lead to considerable reduction in sulfate aerosols, and thus play a major role in improving air quality thereby minimizing its deleterious health impact. The long-term spatial distribution maps of ground-level SO_2 from OMI provide policy-makers with SO_2 pollution monitoring at locations where

ground measurements are not available. Future satellite missions like TEMPO (Tropospheric Emissions: Monitoring Pollution) will provide better coverage of SO_2, and other pollutants, as it will have higher spatial resolution, and hourly frequency over the North American continent during daytime (especially USA and parts of Canada). Also TROPOspheric Monitoring Instrument (TROPOMI) is scheduled to launch in 2017 and will provide daily global coverage of tropospheric SO_2 and other pollutants with a high spatial resolution of 7x7 km^2.

Acknowledgement

We acknowledge the National Aeronautics and Space Administration (NASA) for the availability of OMI SO_2 tropospheric column data. We would like to thank Natural Sciences and Engineering Research Council of Canada (NSERC) for funding support.

References

Bélair, S., Mailhot, J., Girard, C., and Vaillancount, P.: Boundary Layer and Shallow Cumulus Clouds in a Medium-Range Forecast of a Large-Scale Weather System, Mon. Weather Rev., 133, 1938–1960, 2005.

Boys, B. L., Martin, R. V., van Donlelaar, A., MacDonell, R. J., Hsu, N. C., Cooper, M. J., Yantosca, R. M., Lu, Z., Streets, D. G., Zhang, Q., and Wang, S. W.: Fifteen-year global time series of satellite-derived fine particulate matter, Environ. Sci. Technol., 48 (19), 11109-11118, 2014.

Chinn, S., Florey, C. du V., Baldwin, I. G., and Gorgol, M.: The relation of mortality in England and Wales 1969-73 to measurements of air pollution, J. of Epidemiol. and Community Health, 35, 174-179, 1981.

Côté, J., Gravel, S., Méthot, A., Patoine, A., Roch, M., and Staniforth, A.: The operational CMC-MRB Global Environmental Multiscale (GEM) model. Part 1: Design considerations and formulation, Mon. Weather Rev., 126, 1373–1395, 1998.

Dentener, F., Drevet, J., Lamarque, J. F., Bey, I., Eickhout, B., Fiore, A.M., Hauglustaine, D., Horowitz, W.W., Krol, M., Kulshrestha, U.C., Lawrence, M., Galy-Lacaux, C., Rast, S., Shindell, D., Stevenson, D., Van Noije, T., Atherton, C., Bell, N., Bergman, D., Butler, T., Cofala, J., Collins, B., Doherty, R., Ellingsen, K., Galloway, J., Gausee, M., Montanaro, V., Müller, J. F., Pitari, G., Rodriguez, J., Sanderson, M., Solmon, F., Strahan, S., Schultz, M., Sudo, K., Szopa, S., and Wild. O.: Nitrogen and sulfur deposition on regional and global scales: a multimodel evaluation, Global Biogeochem. Cycles., *20*, GB4003, doi:10.1029/2005GB002672, 2006.

Dee, D. P., Uppala, S. M., Simmons, A. J., Berrisford, P., Poli, P., Kobayashi, S., Andrae, U., Balmaseda, M. A., Balsamo, G., Bauer, P., Bechtold, P., Beljaars, A. C. M., van de Berg, L., Bidlot, J., Bormann, N., Delsol, C., Dragani, R., Fuentes, M., Geer, A. J., Haimberger, L., Healy, S. B., Hersbach, H., Holm, E. V., Isaksen, L., Kallberg, P., Kohler, M., Matricardi, M., McNally, A. P., Monge-Sanz, B. M., Morcrette, J.-J., Park, B. –K., Peubey, C., de Rosnay, P., Tavolato, C., Thepaut, J. –N., and Vitart, F.: The ERA-Interim reanalysis: configuration and performance of the data assimilation system, Q. J. R. Meteorol. Soc., 137, 553 – 597, 2011.

Derriennic, F., Richardson, S., Mollie, A., and Lellouch, J.: Short-term effects of sulphur dioxide pollution on mortality in two French cities, Int. J. Epidemiol., 18, 186-197, 1989.

EPA: Air Emissions Inventories, 2016, available online at: https://www.epa.gov/air-emissions-inventories, last accessed on Oct 15, 2016.

Fioletov, V. E., McLinden, C. A., Krotkov, N., Moran, M. D., and Yang, K.: Estimation of SO_2 emissions using OMI retrievals, Geophys. Res. Lett., 38, L21811, doi: 10.1029/2011GL049402, 2011.

Fioletov, V. E., McLinden, C. A., Krotkov, N., Yang, K., Loyola, D. G., Valks, P., Theys, N., Van Roozendael, M., Nowlan, C. R., Chance, K., Liu, X., Lee, C., and Martin, R. V.: Application of OMI, SCIAMACHY, and GOME-2 satellite SO_2 retrievals for detection of large emission sources, J. Geophys. Res. Atmos., 118, 11,399-11,418, 2013.

Fioletov, V. E., McLinden, C. A., Krotkov, N., and Li, C.: Lifetimes and emissions of SO_2 from point sources estimated from OMI, Geophys. Res. Lett., 42, 1969–1976, 2015.

Fioletov, V. E., McLinden, C. A., Krotkov, N., Li, C., Joiner, J., Theys, N., Carn, S., and Moran, M. D.: A global catalogue of large SO_2 sources and emissions derived from the Ozone Monitoring Instrument, Atmos. Chem. Phys., 16, 11497-11519, 2016.

Gong, W., Makar, P. A., Zhang, J., Milbrandt, J., Gravel, S., Hayden, K. L., Macdonald, A. M., and Leaith, W. R.: Modelling aerosol-cloud-meteorology interaction: a case study with a fully coupled air quality model (GEM-MACH), Atmos. Environ., 115, 695-715, 2015.

Hand, J. L., Schichtel, B. A., Malm, W. C., and Pitchford, M. L.: Particulate sulfate ion concentration and SO_2 emission trends in the United States from early 1990s through 2010, Atmos. Chem. Phys., 12, 10353-10365, 2012.

Hatzakis, A., Katsouyanni, K., Kalandidi, A., Day, N., and Trichopoulos, D.: Short-term effects of air pollution on mortality in Athens, Int. J. Epidemiol., 15(1), 73-81, 1986.

Intergovernmental Panel on Climate Change (2013), Climate Change 2013: The Physical Science Basis. Contribution of Working Group I to the Fifth Assessment Report of the Intergovernmental Panel on Climate Change, edited by T. F. Stocker et al., 1535 pp., Cambridge Univ. Press, Cambridge, U. K., and New York.

Kelly, J., Makar, P. A., and Plummer, D. A.: Projections of mid-century summer air-quality for North America: effects of changes in climate and precursor emissions, Atmos. Chem. Phys., 12, 5367–5390, 2012.

Kharol, S. K., Martin, R. V., Philip, S., Boys, B., Lamsal, L. N., Jerrett, M., Brauer, M., Crouse, D. L., McLinden, C., and Burnett, R. T.: Assessment of the magnitude and recent trends in satellite-derived ground-level nitrogen dioxide over North America, Atmos. Environ., 118, 236-245, 2015.

Krotkov, N. A., Carn, S. A., Krueger, A. J., Bhartia, P. K., and Yang, K.: Band residual difference algorithm for retrieval of SO2 from the Aura Ozone Monitoring Instrument (OMI), IEEE Trans. Geosci. Remote Sens., 44(5), 1259–1266, 2006.

Krotkov, N. A., McLinden, C. A., Li, C., Lamsal, L. N., Celarier, E. A., Marchenko, S. V., Swartz, W. H., Bucsela, E. J., Joiner, J., Duncan, B. N., Boersma, K. F., Veefkind, J. P., Levelt, P. F., Fioletov, V. E., Dickerson, R. R., He, H., Lu, Z., and Streets, D. G.: Aura OMI observations of regional SO_2 and NO_2 pollution changes from 2005 to 2015, Atmos. Chem. Phys., 16, 4605–4629, 2016.

Krzyzanowski, M., and Wojtyniak, B.: Ten-year Mortality in Sample of an adult Population in relation to air pollution, J. Epidemiol. Community Health., 36(4), 262-268, 1982.

Lamsal, L. N., Martin, R. V., van Donkelaar, A., Steinbacher, M., Celarier, E. A., Bucsela, E., Dunlea, E. J., and Pinto, J. P.: Ground-level nitrogen dioxide concentrations inferred from the satellite-borne Ozone Monitoring Instrument, J. Geophys. Res., 113, D16308, doi:10.1029/2007JD009235, 2008.

Lee, C., Martin, R. V., van Donkelaar, A., Lee, H., Dickerson, R. R., Hains, J. C., Krotkov, N., Richter, A., Vinnikov, K., and Schwab, J. J.: SO_2 emissions and lifetimes: Estimates from inverse modeling using in situ and global, space-based (SCIAMACHY and OMI) observations, J. Geophys. Res., 116, D06304, doi:10.1029/2010JD014758, 2011.

Lee, C. J., Martin, R. V., Henze, D. K., Brauer, M., Cohen, A., and van Donkelaar, A.: Response of global particulate-matter-related mortality to changes in local precursor emissions, Environ. Sci. Technol., 49, 4335–4344, 2015.

Lelieveld, J., Evans, J. S., Fnais, M., Giannadaki, D., and Pozzer, A.: The contribution of outdoor air pollution sources to premature mortality on a global scale, Nature, 525, 367-371, 2015.

Levelt, P. F., van den Oord, G. H. J., Dobber, M. R., Malkki, A., Visser, H., de Vries, J., Stammes, P., Lundell, J. O. V., and Saari, H.: The Ozone Monitoring Instrument, IEEE Trans. Geosci. Remote Sens., 44, 1093-1101, 2006.

Li, C., Joiner, J., Krotkov, N. A., and Bhartia, P. K.: A fast and sensitive new satellite SO_2 retrieval algorithm based on principal component analysis: Application to the ozone monitoring instrument, Geophys. Res. Lett., 40, doi:10.1002/2013GL058134, 2013.

McLinden, C, A., Fioletov, V. E., Boersma, K. F., Kharol, S. K., Krotkov, N. A., Lamsal, L., Makar, P. A., Martin, R. V., Veefkind, J. P., and Yang, K.: Improved satellite retrievals of NO_2 and SO_2 over the Canadian oil sands and comparisons with surface measurements, Atmos. Chem. Phys., 14, 3637-3656, 2014.

McLinden, C. A., Fioletov, V., Shephard, M. W., Krotkov, N., Li, C., Martin, R. V., Moran, M. D., and Joiner, J.: Space-based detection of missing sulfur dioxide sources of global air pollution, Nature-Geoscience, 9, 496-500, 2016a.

McLinden, C, A., Fioletov, V. E., Krotkov, N. A., Li, C., Boersma, K. F., and Adams, C.: A decade of change in NO_2 and SO_2 over the Canadian Oil Sands as seen from space, Environ. Sci. Technol., 50, 331-337, 2016b.

Moran, M. D., Menard, S., Talbot, D., Huang, P., Makar, P. A., Gong, W., Landry, H., Gravel, S., Gong, S., Crevier, L.-P., Kallaur, A., and Sassi, M.: Particulate-matter forecasting with GEM-MACH15, a new Canadian operational air quality forecast model. In: Steyn, D. G. Rao, S.T. (Eds.), Air Pollution Modelling and its Application XX. Springer, Dordrecht, 289–293, 2010.

Nowlan, C. R., Liu, X., Chance, K., Cai, Z., Kurosu, T. P., Lee, C., and Martin, R. V.: Retrievals of sulfur dioxide from the Global Ozone Monitoring Experiment 2 (GOME-2) using an optimal estimation approach: Algorithm and initial validation, J. Geophys. Res., 116, D18301, doi:10.1029/2011JD015808, 2011.

Nowlan, C. R., Martin, R. V., Philip, S., Lamsal, L. N., Krotkov, N. A., Marais, E. A., Wang, S., and Zhang, Q.: Global dry deposition of nitrogen dioxide and sulfur dioxide inferred from space-based measurements, Global Biogeochem. Cycles, 28, doi:10.1002/2014GB004805, 2014.

NPRI: National Pollutant Release Inventory datasets, 2017, available online at: http://www.ec.gc.ca/inrp-npri/default.asp?lang=En&n=0EC58C98-, last accessed on Mar 01, 2017.

Philip, S., Martin, R. V., van Donkelaar, A., Lo, J. W. –H., Wang, Y., Chen, D., Zhang, L., Kasibhatla, P. S., Wang, S., Zhang, Q., Lu, Z., Streets, D. G., Bittman, S., and Macdonald, D. J.: Global chemical composition of ambient fine particulate matter for exposure assessment, Environ. Sci. Technol., 48, 13060-13068, 2014.

van Donkelaar, A., Martin, R. V., Leaitch, W. R., Macdonald, A. M., Walker, T. W., Streets, D. G., Zhang, Q., Dunlea, E. J., Jimenez, J. L., Dibb, J. E., Huey, L. G., Weber, R., and Andreae, M. O.: Analysis of aircraft and satellite measurements from the Intercontinental Chemical Transport Experiment (INTEX-B) to quantify long-range transport of East Asian sulfur to Canada, Atmos. Chem. Phys., 8, 2999-3014, 2008.

van Donkelaar, A., Martin, R. V., Brauer, M., Kahn, R. A., Levy, R. C., Verduzco, C., and Villeneuve, P. J.: Global estimates of ambient fine particulate matter concentrations from satellite-based aerosol optical depth: development and application, Environ. Health Perspec., doi: 10.1289/ehp.0901623, 118(6), 2010.

Vet, R., Artz, R. S., Carou, S., Shaw, M., Ro, C.-U., Aas, W., Baker, A., Bowersox, V. C., Dentener, F., Galy-Lacaux, C., Hou, A., Pienaar, J. J., Gillett, R., Forti, M. C., Gromov, S., Hara, H., Khodzher, T., Mahowald, N. M., Nickovic, S., Rao, P. S. P., and Reid, N. W.: A global assessment of precipitation chemistry and deposition of sulfur, nitrogen, sea salt, base cations, organic acids, acidity and pH, and phosphorus, Atmos. Environ., 93, 3-100, 2014.

Yang, K., Krotkov, N. A., Krueger, A. J., Carn, S. A., Bhartia, P. K., and Levelt, P. F.: Retrieval of large volcanic SO_2 columns from the Aura Ozone Monitoring Instrument: Comparison and limitations, J. Geophys. Res., 112, D24S43, doi:10.1029/2007JD008825, 2007.

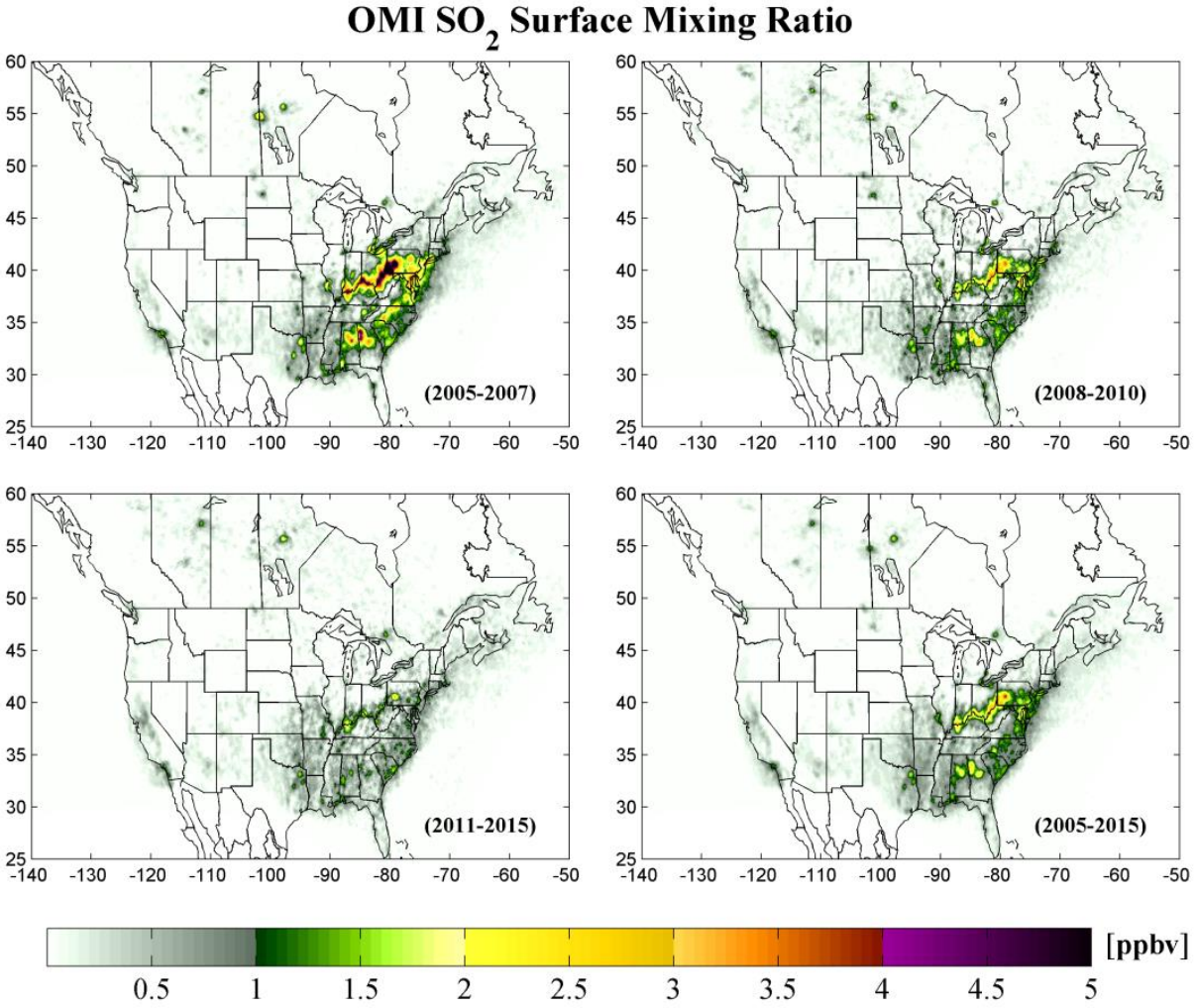

Figure 1: Spatial distribution of mean OMI-derived ground-level SO_2 mixing ratio over North America for the period of 2005-2007, 2008-2010, 2011-2015 and 2005-2015.

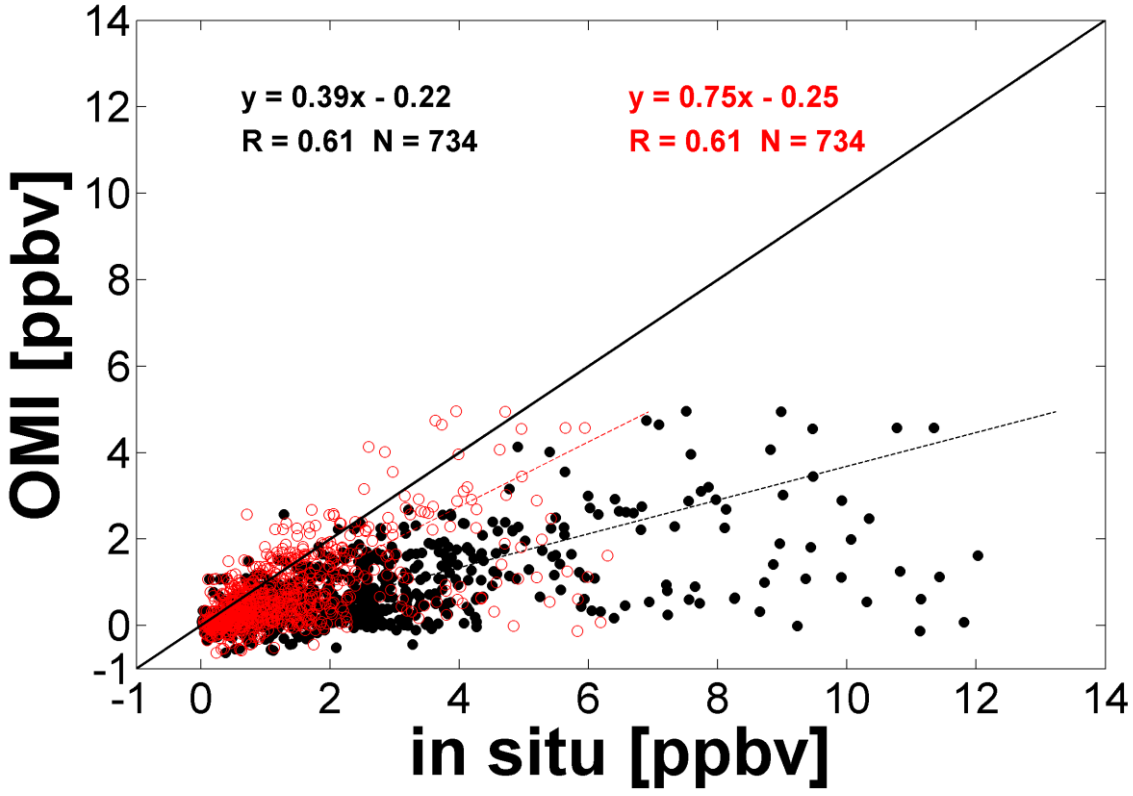

Figure 2: Scatter plot of the annual mean OMI-derived ground-level SO_2 versus collocated in-situ measurements for the years of 2005-2015. Filled black circles represent the original in-situ values, and red circles represent the comparison with spatially inhomogeneity adjusted in-situ values.

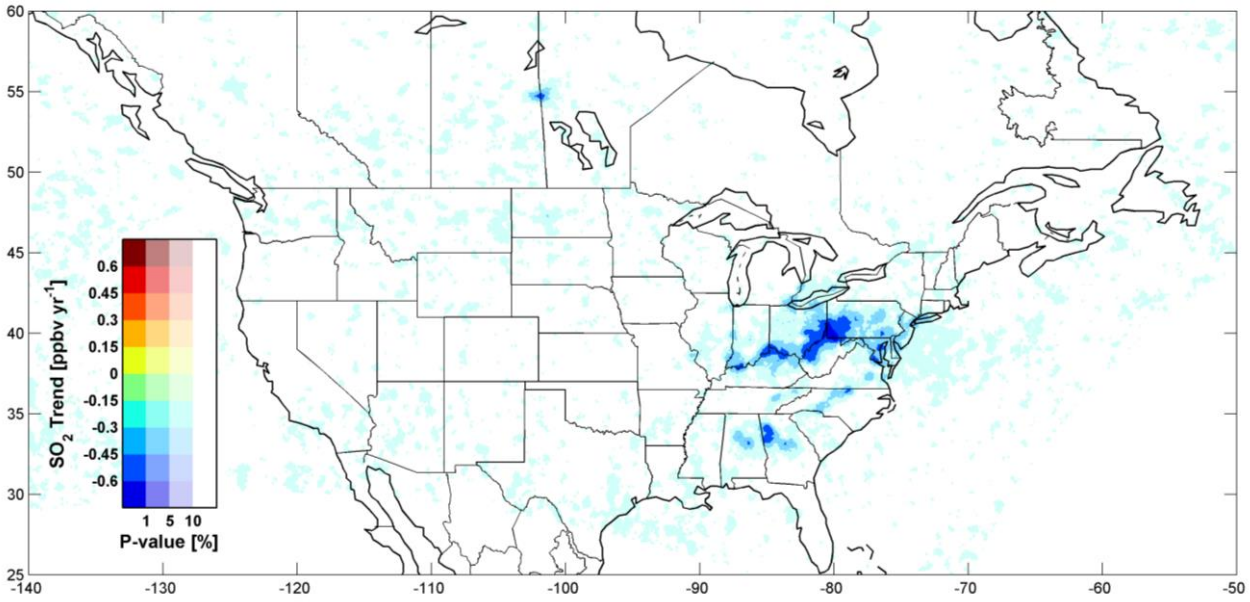

Figure 3: Spatial distribution of OMI-derived surface SO_2 trend at $0.1^o \times 0.1^o$ over North America for the year of 2005-2015. Statistical significance is shown in the form of a two sided P-value, tested against null being zero trend.

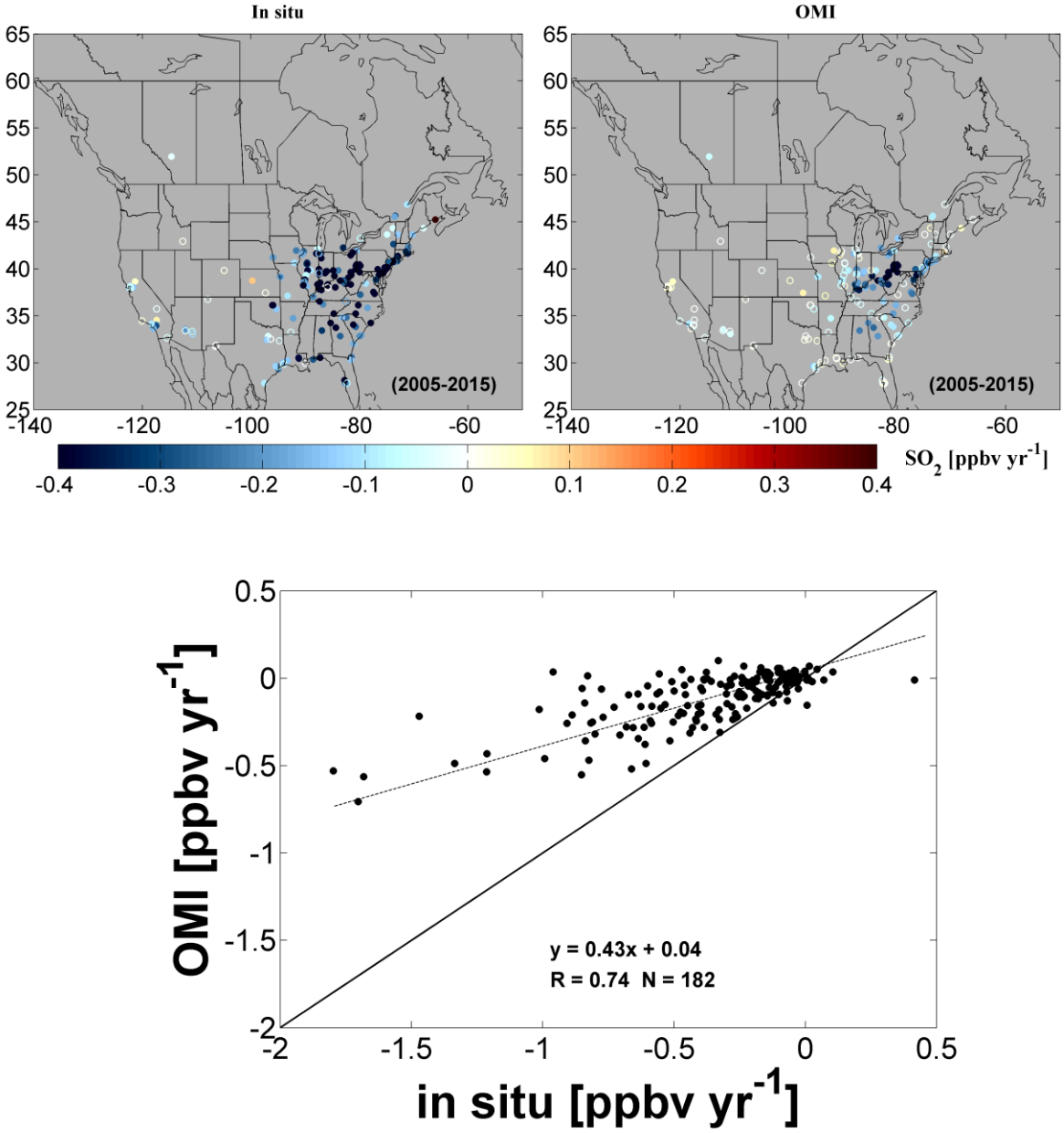

Figure 4: Trends in ground-level SO_2 for the period of 2005-to-2015. The top row shows trends inferred from in-situ measurements at OMI overpass and from OMI for the period of 2005-2015. The filled circle represents where trend p-value < 0.05 and trend p-values > 0.05 are shown as empty circle. The bottom panel contains scatter plots of trends for the period of 2005-2015.

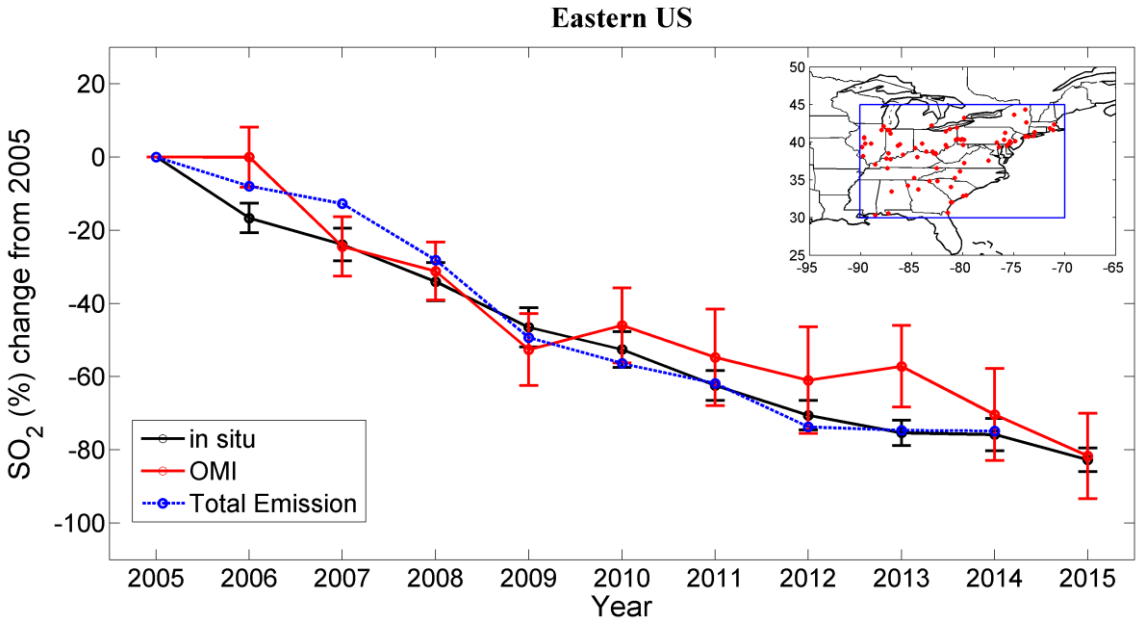

Figure 5: Percent change in ground-level SO_2 mixing ratio from 2005 over Eastern US and southern Ontario, Canada. The in-situ and OMI ground-level SO_2 percent change are shown in black and red color, respectively. Blue circles show changes in total SO_2 emissions. The locations of in-situ measurement stations over Eastern US and southern Ontario, Canada (blue box) are shown in the inset map. The error bars represent the 1-standard error of the mean.

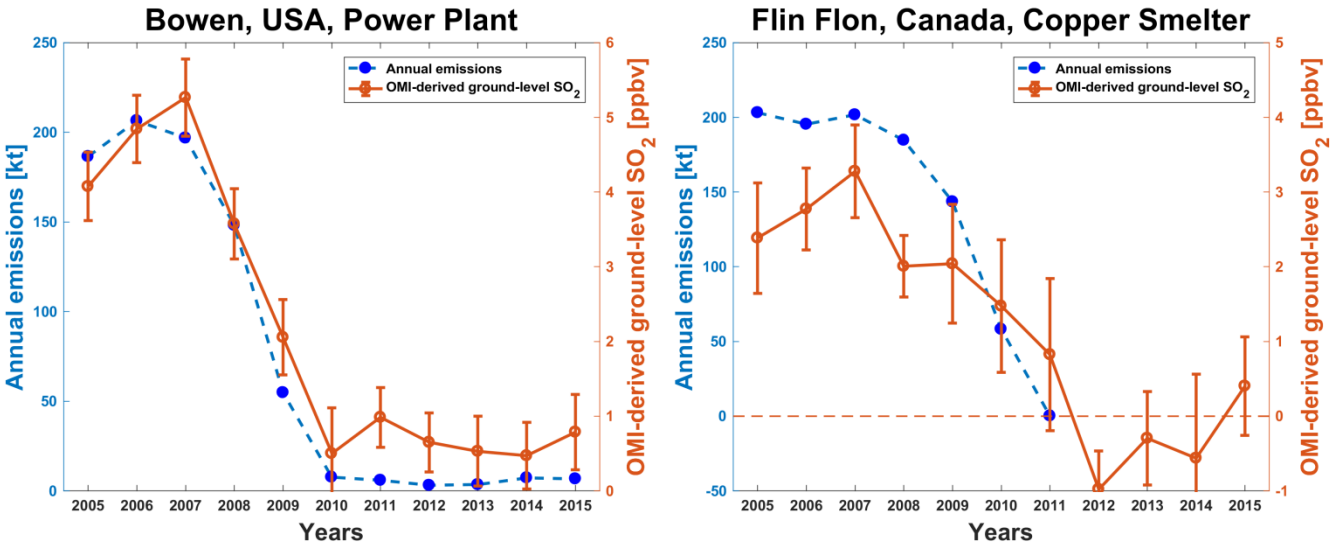

Figure 6: Time series of bottom-up annual SO_2 emissions and OMI-derived ground-level SO_2 concentration for Bowen power plant (34.13° N, 84.92° W), USA, and Flin Flon copper smelter (54.77° N, 101.88° W), Canada. The dashed orange line represents the zero line in Flin Flon, Canada plot. Bottom-up SO_2 emissions data are not available after 2011 due to closer of Flin Flon copper smelter. The error bars represent the 1-standard error of the mean.

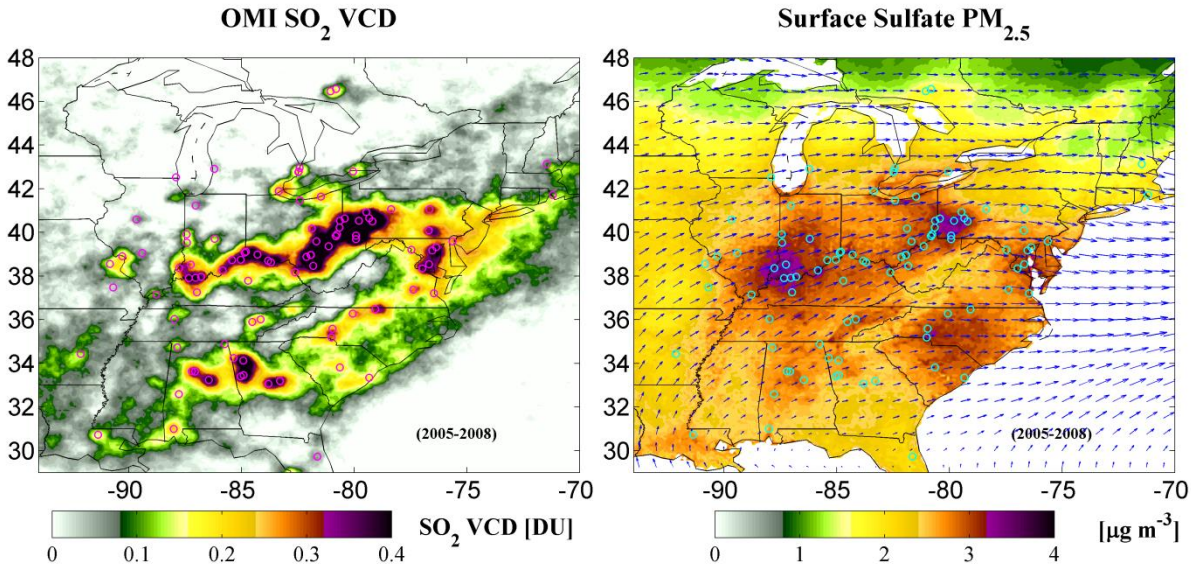

Figure 7: Spatial distribution of satellite derived SO_2 vertical column density (VCD) and sulfate $PM_{2.5}$ mass concentration over eastern US and southern Ontario, Canada. The power plant locations overlaid on both panels are shown as circle. ECMWF model derived ground-level winds are overlaid on sulfate $PM_{2.5}$ mass concentration map are shown with arrows.